NOVEL PERYLENE IMIDES FOR SOLID STATE DYE-SENSITIZED SOLAR CELLS

Henry Petman

Bachelor's thesis
May 2016
Degree Programme in Laboratory Sciences

ABSTRACT

Tampereen ammattikorkeakoulu
Tampere University of Applied Sciences
Degree Programme in Laboratory Sciences

PETMAN, HENRY:
Novel perylene imides for solid-state dye-sensitized solar cells

Bachelor's thesis 33 pages, appendices 3 pages
May 2016

Dye-sensitized solar cells are an attractive technology emerging on the market because of the advantages with respect to the traditional inorganic silicon based cells, such as low-cost materials and fabrication processes, flexibility, light weight. Some challenges still remain in the field of research before the cells can be further commercialized, such as the optimization of the fabrication processes to enhance the overall cell performance, the long-term stability, the upscaling from laboratory-size to large-scale modules.

Aim of this Thesis was to analyze the performance of solar cells based on a novel organic dye compounds synthesized at Tampere University of Technology (TUT), Department of Chemistry and Bioengineering. Experimental work and measurements were done during training period on spring 2016, while the devices were fabricated earlier in summer 2015.

Solar cells were manufactured with a commercially available ruthenium dye, and were compared to devices including the perylene-based dye synthesized at TUT. The photovoltaic devices were measured regularly over half year period under simulated illumination to investigate their ability to provide electricity through an external circuit. From the I-V characteristics of the solar cells, the power conversion efficiencies and other important parameters could be calculated in order to compare their performance and the aging of the devices stored in darkness in ambient conditions. In the end, results were very promising for the home-made compound to be studied even more.

TIIVISTELMÄ

Tampereen ammattikorkeakoulu
Tampere University of Applied Sciences
Laboratorioala

PETMAN, HENRY:
Novel perylene imides for solid-state dye-sensitized solar cells

Opinnäytetyö 33 sivua, liitteet 3 sivua
Maaliskuu 2016

Väriaineherkisteyt aurinkokennotovat houkutteleva uusi teknologia johtuen sen eduista perinteisiin silikonipohjaisiin aurinkokennoihin verrattuna, kuten halvemmat materiaalit sekä valmistusprosessit, joustavuus sekä kevytrakenteisuus. Joitakin haasteita kuitenkin on vielä tutkittavana ennenkuin näitä aurinkokennoja pystytään hyödyntämään eteenpäin, kuten valmistusprosessin optimointi, pitkäkestoisuus, sekä skaalaus laboratoriokoosta suuremman koon kennoihin.

Opinnäytetyön tavoitteena oli analysoida TTY:llä valmistettujen orgaanisten väriainemolekyylien suorituskykyä aurinkokennoissa. Työn kokeellinen osuus sekä mittaukset tehtiin keväällä 2016 aurinkokennoilla jotka oli valmistettu aiemmin kesällä 2015.

Aurinkokennoja valmistettiin yleisesti käytössä olevalla rutenium –väriaineella herkistettynä sekä omatekoisella peryleenipohjaisella väriaineella herkistettynä ja näiden suorituskykyä ja elinkaarta verrattiin toisiinsa. Kennoja mitattiin säännöllisin väliajoin puolen vuoden ajalla simuloidulla auringonvalolla ja niistä tutkittiin niiden kykyä antaa sähköä virtapiiriin. Virta-jännitekäyristä laskettiin kennojen hyötysuhde sekä muita tärkeitä parametreja ja niitä verrattiin toisiinsa. Tulokset vaikuttivat lupaavilta omatekoisen väriaineen kannalta ja sitä on aihetta tutkia lisää.

Key words: solar cell, organic, solid state, ssdssc

CONTENTS

Key words: aurinkokenno, orgaaninen, kiinteän tilan, ssdssc

ABBREVIATIONS AND TERMS

DSSC	Dye-sensitized solar cell
eV	Electron volt
FF	Fill factor
FTO	Fluorine-doped tin oxide
HOMO	Highest occupied molecular orbital
HTM	Hole transporting material
I	Electric current
Isc	Short circuit current
J	Current density
Jsc	Short circuit current density
LUMO	Lowest unoccupied molecular orbital
N719	Ruthenizer 535-bisTBA
OPV	Organic photovoltaic
PMI	perylene monoimide
P3HT	Poly(3-hexylthiophene-2,5-diyl)
PCBM	Phenyl-C61-butyric acid methyl ester
P_{in}	Input power
P_{max}	power at maximum power point
ssDSSC	Solid-state dye-sensitized solar cell
TAMK	Tampere University of Applied Sciences
TUT	Tampere University of Technology
V_{oc}	Open circuit voltage
ZA96	9-octyl-5,13-di(pyrrolidin-1-yl)-1Hisochromeno[6',5',4':10,-5,6]anthra[2,1,9-def]isoquinoline-1,3,8,10(9H)-tetraone

1 INTRODUCTION

Solar cells are intensively and widely researched, since they represent an attractive technology to meet the energy needs. In fact, the world demand for energy grows rapidly and continuously, and at the same time fossil fuels resources are running out. Moreover, the combustion of fossil fuels pollutes the environment with harmful substances. The working principle of solar cells is based on the conversion of the energy coming from sun as photons into electrons that can be injected to an electrical circuit. The first commercial applications of photovoltaics, namely the inorganic Silicon-based solar cells, date back to 1970's and the dye-sensitized solar cell research was begun in the 1990's (Figure 1). The need for cheaper and more environmental friendly starting materials has led to interest in researching alternative technologies for producing solar cells. Currently an enormous focus is on hybrid inorganic-organic solar cell, which have proven to show interesting performances and to be at the same time the most convenient in terms of materials and fabrication costs. (IEA 2014)

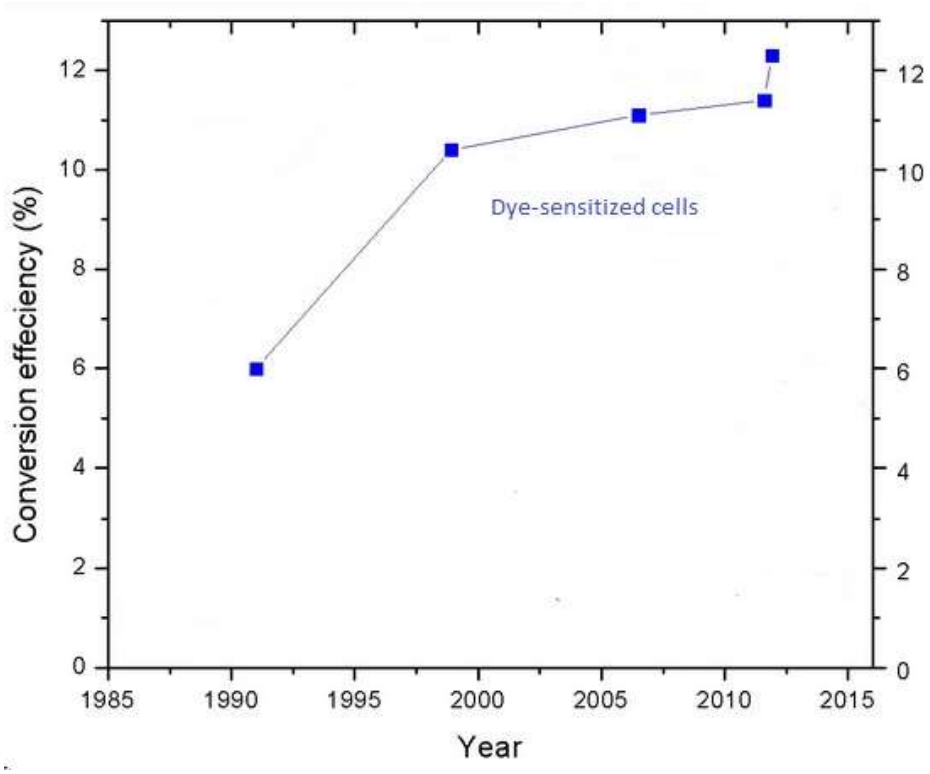

FIGURE 1. Development of dye-sensitized solar cells technologies

There is much more solar energy reaching the earth's surface than the humankind currently uses. To convert solar energy into electricity it is not always needed to have highly efficient devices, but sometimes it is more convenient to connect in parallel many solar cells with lower efficiencies, such as organic solar cells. Commercial inorganic silicon cells suffer from huge power losses if even one cell in the parallel series is dusty or clouded from sun, leading up to 90 % efficiency loss (DTU 2016). On the other hand, organic cells connected in parallel perform at almost full power, even when a big portion of light is blocked for some of the cells (Figures 2 and 3).

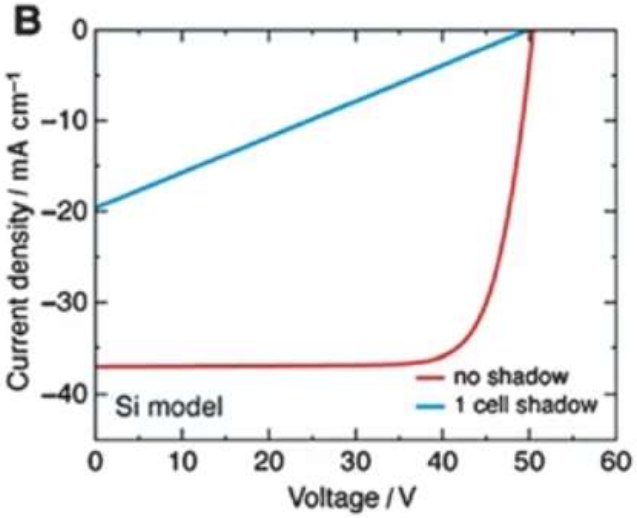

FIGURE 2. Comparison of inorganic solar cell performance when part of the cell battery is clouded (Technical University of Denmark 2016, edited)

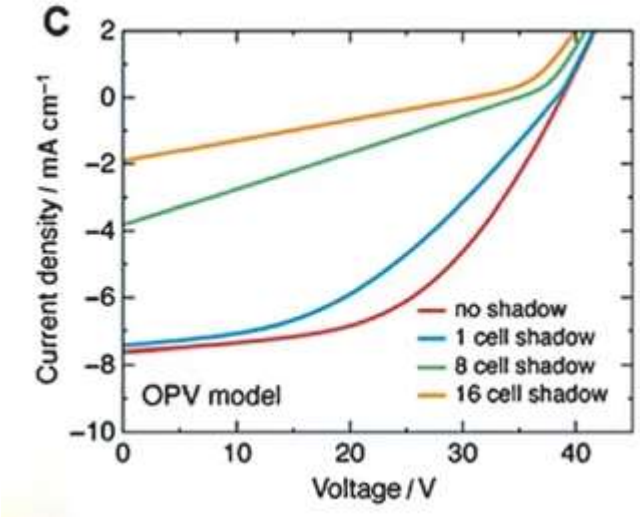

FIGURE 3. Comparison of organic solar cell performance when part of the cell battery is clouded (Technical University of Denmark 2016, edited)

Such advantages of organic solar cells explain the interest on this technology. Moreover, the growing number of publications per year shows that lots of effort is made to optimize these new cell types, with the final goal of strengthening and widening their place in the market. All work in this Thesis was carried out at the Department of Chemistry and Bioengineering, Tampere University of Technology, under the supervision of Academy post-doctoral researcher Paola Vivo.

2 THEORY BACKGROUND

2.1. Photovoltaic effect

Photovoltaic effect is the phenomenon behind the solar cells functioning, i.e. the conversion of sunlight into electricity. A molecule absorbs the energy of a photon coming from sun, which excites an electron of its outer electron shell. With this energy the electron is capable of moving from its normal position into an electrical circuit and generate current (Halls 2001, 377–445) (Figure 4).

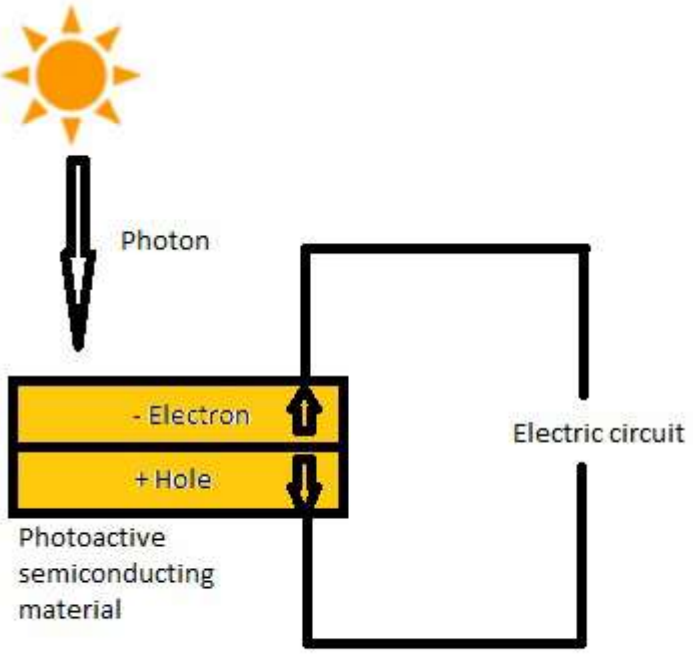

FIGURE 4: Generation of current from solar power

If the powered circuit is open, the electrons under sunlight illumination cannot pass through and only voltage can be observed from the cell, namely the open circuit voltage, V_{OC}. In case of closed circuit with zero ohmic load the maximal circuit current can be measured, which is termed as short circuit current, I_{SC}. These are only theoretical parameters used for comparison of cell characteristics, since neither condition is able to provide power to an external device.

Fill factor (*FF*) is the ratio of the maximum power that can be drawn from the device (P_{MAX}) and the theoretical power, as in Eq. 1:

(1)

FF is directly related to the series and shunt resistance of the cell. Higher fill factors are achieved by increasing the shunt resistance and decreasing the series resistance. A larger *FF* is desirable, and corresponds to a more "square-like" shape of the I–V curve.

The power conversion efficiency of the device (η) can be calculated from the defined parameters. η is the ratio of the maximum generated power (P_{MAX}) to the incident optical power reaching the solar cell (P_0). Hence, η can be expressed as follows (Eq. 2). (Vivo 2010)

(2)

2.2. Different types of solar cells technologies

Solar cell technologies mostly revolve around semiconductor material properties, both organic and inorganic. Photovoltaic cells can be classified as first, second and third generation. First generation are the traditional thick wafer-based silicon solar cells, with crystalline silicon being the light absorbing and charge separating material. Second generation consists of thin-film based technologies which are cheaper, much thinner and lower weight, flexible but less efficient than first generation. Examples of this type are amorphous silicon and Cd-Se cells (DTU 2016). Third generation cells are further explained in the next chapter.

The first two generations have the largest commercial applications, but some expamples of organic or dye-sensitized modules have also already appeared on the market. This so-called third generation of photovoltaics promise to combine the best parts of earlier generations' cells, i.e. the low cost and high efficiency. The third generation photovoltaics are based on hybrid organic-inorganic technologies such as perovskite and dye-sensitized cells, which use organometallic compounds and also fully organic dyes.

Since they are an emerging technology and haven't had so many years of investigation as older technologies, many problems are still to be solved, such as the stability of the cells. In fact, most of the new cells which have been developed with high performance as priority, e.g. perovskite-based solar cells, usually suffer from very poor lifetimes which makes them unconvenient for any real-life applications. A very few of the novel cell types can last even days under solar illumination. It is thus necessary to search for new materials with improved photostability and which are able to tolerate moisture and oxygen without major worsening of their performances. Alternatively, encapsulation solutions for the devices should be developed (DTU 2016).

2.3. Solid state dye sensitized solar cell

Solid state dye sensitized solar cells (ssDSSC) are a low-cost emerging technology with many potential applications in the solar energy field because of their advantages in cost-effectiveness and stability properties compared to dye-sensitized solar cells. In fact, the lifetime of DSSCs is limited by the encapsulation of the liquid electrolyte, and its inertness towards the iodine of which both problems are solved in the newer solid state model (Merhari 2009, 305-306).

A ssDSSC differs from a traditional DSSC in the hole conductor for the dye regeneration: a solid-state hole transporting material (HTM) is here employed instead of the liquid electrolyte of DSSC. This leads to enhanced durability in terms of degradation and performance over time. The main advantage of ssDSSC is their robust efficiency: they can operate for even thousands of hours without significant losses in terms of efficiency according to measurements performed. Compared to many other cells technologies and some novel research cells this is a rare feature and it motivates further current study of this technology.

This Thesis aims to investigate a novel metal-free dye compound synthesized at the Department of Chemistry and Bioengineering (KEB), Tampere University of Technology (TUT), as a possible sensitizer for solid-state dye sensitized solar cells. A comparison of its characteristics with the well-known and widely used commercial Ruthenium-dye molecule available was done, with a special focus on the aging of the solar cells in time.

2.3.1 Different layers in solid state dye-sensitized solar cells

Solid state dye-sensitized solar cells comprise several different layers (Figure 5), which can be described as follows: one of the two cell electrodes is the fluorine-doped tin oxide (FTO) layer, which acts as conducting layer for electrons; on top of that there is the compact titania layer, i.e. the electron transporting layer in which electrons can move but holes cannot; after which comes the dye sensitized mesoporous titania layer which is responsible of the photoinduced separation of electron and holes upon light excitation. Electron and holes travel in opposite directions. Electrons travel towards the compact titania layer and are collected at the FTO layer, while holes are transported through the HTM, unless the charge is recombined before. Finally, holes are collected at the cell cathode, which is typically a silver electrode thermally evaporated on top of the HTM. Electrons and holes that are successfully separated generate voltage between the electrodes of solar cell, i.e. FTO and silver.

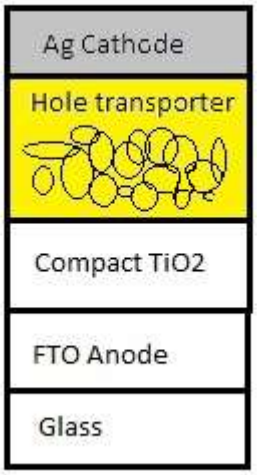

FIGURE 5. Different layers of ssDSSC

In order to increase the efficiency over the 2nd generation solar cells, it has been shown that by arranging the light absorbing dye on a FTO-coated “mesoporous” titania layer, the efficiency of the cell will increase dramatically by increasing the absorbing surface area and number of molecules capable of donating electrons. Most of the novel solar

cells architectures have been developed in this way, although their mass-scale production is not so easy to achieve (DTU 2016).

2.3.2 Perylene imides

Perylene imides are a class of organic compounds with a very high visible light absorption, high stability and electron pair accepting capability. They act as antenna, similarly to chrolophyll (Figure 6) in plants: they absorb the energy of photons from sun at different wavelengths corresponding to their color. The skeleton of the molecule is large, thus there is much space for substitution to modify the properties of the compound for different needs such as absorption and solubility (Saarinen 2015).

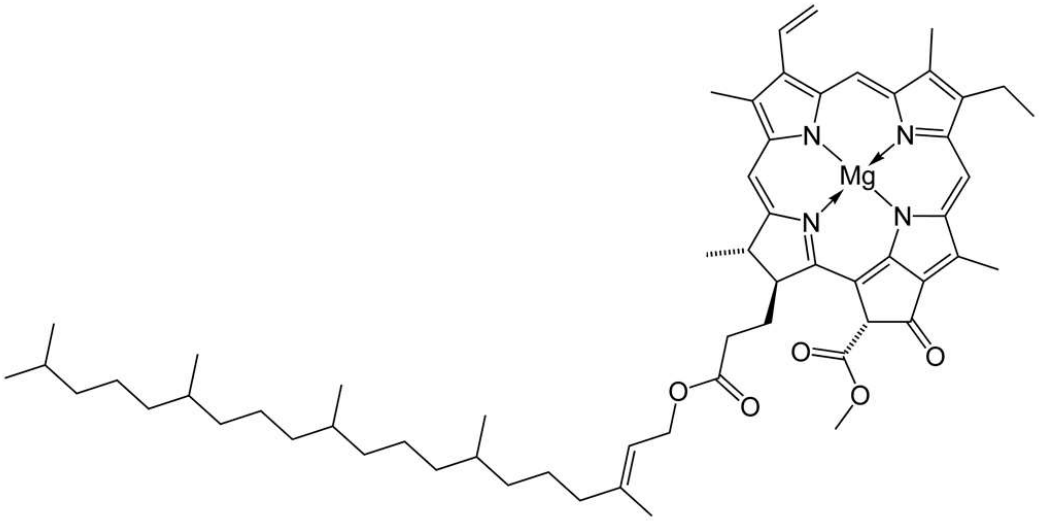

FIGURE 6. Chlorophyll-a molecular structure

In solar cells, perylene imides are used as sensitizer molecules for the mesoporous titanium dioxide layer, facilitating the movement of electrons within the cell towards the FTO-electrode and thus increasing the final efficiency. Earlier experiments made for comparison show that with the perylene coating of titania layer the efficiency is 20 times greater than without the dye molecule in ssDSSC cells (Saarinen 2015).

FIGURE 7. ZA96 molecular structure

Perylene compound ZA96, blue in color and named after its creator Dr. Zafar Ahmed of TTY, (Figure 7) was chosen in this Thesis as one promising candidate among several dyes with different substitutions. By taking into account the previous experiments at KEB on several perylene dyes, i.e. the voltammetry experiments to determine the HOMO/LUMO energy levels of the compounds, the fundamental spectroscopic characterization and also some previous solar cell experiments, it was concluded that ZA96 is the best option, among the perylene monoimides available at TUT, to compete with the high performance industrial standard ruthernium red color dye, N719.

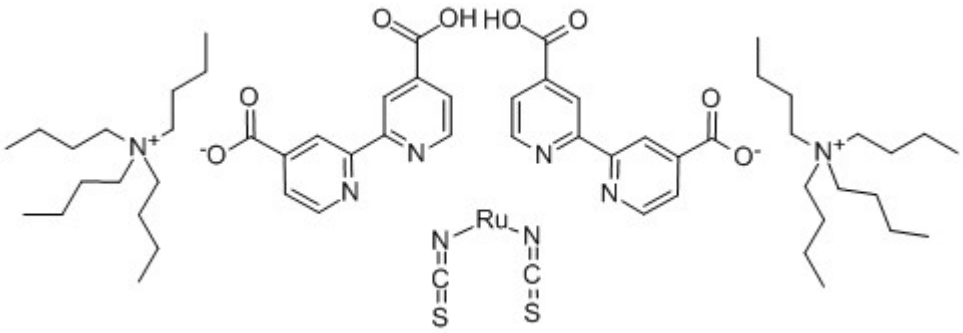

FIGURE 8. N719 molecular structure (ChemicalBook Inc. 2016)

Ruthenium element used in N719 (Figure 8) is a very rare and expensive (Bentor 2016) element like platinum so there is great need for finding alternative replacements for it, metal-containing and metal-free. Ruthenium-dyes show as well very good stability in ambient air conditions, and are widely used in highly efficient solar cells. In this Thesis, the aim is to introduce a much cheaper fully organic dye molecule, ZA96, and compare its properties in solar cells with those of the commercial ruthenium dye, N719.

3 EXPERIMENTAL

3.1. Materials and methods

All solar cells were fabricated onto 2x2 cm substrates consisting of glass slides, with one side fully covered with conducting fluorine-doped tin oxide, the work was conducted in a cleanroom. The FTO substrates were commercially available and supplied by Solems. The dye was either the perylene (ZA96) or the Ru-dye (N719). Compact and mesoporous layer were fabricated immediately after each other in order to reduce particle contamination and to make sure the interface between these layers is clean as possible to avoid short circuiting.

The basic structures for the cells were:

FTO|Compact TiO_2|Mesoporous TiO_2|ZA96| P3HT |Ag
FTO|Compact TiO_2|Mesoporous TiO_2|N719| P3HT |Ag

3.1.1 Acid etching

In order to avoid short-circuiting when contacting the top-electrode, FTO was partly removed from the substrates by acid etching treatment. The areas where FTO is desired were protected by kapton tape. The parts where the removal of FTO is aimed had to be etched by dropping zinc powder and spreading 4M hydrochloric acid on top (Picture 1). The acid was brushed with toothbrush for a more uniform distribution. Finally, the substrate was rinsed with ethanol to neutralize the acidity.

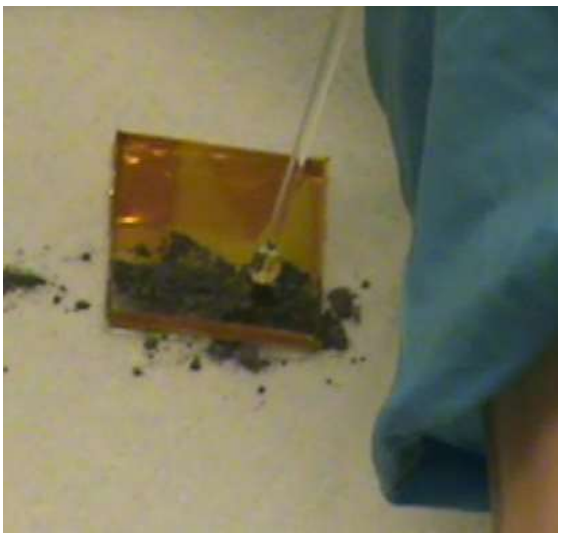

PICTURE 1. Acid etching in action

3.1.2 Cleaning of substrates

After etching, the substrates were thoroughly cleaned in multiple ultrasonic baths in glass containers by following a well-know procedure. The cleaning steps are listed as follows:

1. Brushing the substrates with Hellmanex solution 2 % in milli-Q water with toothbrush
2. Ultrasonic bath with Hellmanex 2% solution for 15 minutes
3. Rinsing the plates with abundant milli-Q water and ethanol
4. Ultrasonic bath with isopropanol (IPA) solution for 15 minutes
5. Drying the substrates under nitrogen flow

Finally, the glass substrates were placed in UV-ozone cleaner for 10 minutes before fabrication of the layers, to remove any organic contaminant.

3.1.3 Spin-coating

Spin-coater (Picture 2) works by holding the substrate under vacuum and dropping the solution of the material wanted to be deposited in the middle of the plate. The substrate is then spinned and the solution will spread evenly because of centrifugal forces.

After taking out from UV-ozone cleaner, the clean glass substrates were masked with kapton tape to limit the active area only to the central part of the plate. Both thin-film titania layer and also the mesoporous titania layer were deposited by spin-coating and the films where then sintered at high temperatures. The hole-transport material, P3HT, was also spin-coated after deposition of the dye layer.

PICTURE 2. Spin-coater machine used in the experiments

Program used in the spin-coater was different for compact- and mesoporous-, and P3HT layers, since the solutions were of different viscosity, concentration and required different temperatures afterprocessing. The parameters shown in following tables 1, 2 and 3 were programmed for each layer separately:

TABLE 1. Spin-coater program for compact TiO_2 layer

Acceleration:	3000 rpm/s
Speed:	3000 rpm
Time:	30 s
Volume:	70 µl
Solvent:	anhydrous IPA
Concentration:	N/A

Precursor solution for compact layer was made by adding solution 1 prepared as below to solution 2, also shown below, dropwise under stirring.

Solution 1:

1.25 ml of anhydrous 2-propanol

175 µl of titanium isopropoxide

Solution 2:

1.25 ml anhydrous 2-propanol

17.5 µl of 2 M HCl

After spin-coating the compact layer, the mesoporous layer was spin-coated immediately after 10 minutes of drying at 120 °C and cooling down.

TABLE 2. Spin-coater program for mesoporous 30-NR-D type TiO_2

Acceleration:	2000 rpm/s
Speed:	4000 rpm
Time:	10 s
Volume:	50 µl
Solvent:	anhydrous IPA
Concentration:	0,8 g/ml

Mesoporous layer was dried at 100 °C for 8 minutes after which the substrates were placed in furnace and sintered.

P3HT layer was spin-coated only after deposition of the dye layer, program shown below.

TABLE 3. Spin-coater program for P3HT

Acceleration:	N/A
Speed:	2000 rpm
Time:	30 sec
Volume:	60 ul
Solvent:	Chlorobenzene
Concentration:	20 mg/mL

After spin-coating, the plates were annealed at 140 °C for 20 minutes under vacuum. Once the annealing was completed, the organic film was removed from the part of the plates where the electric contacts will be placed. This was done by using cotton swabs dipped in chloroform.

3.1.4 Sintering

In order to form the correct crystal structure, the titania films were placed in a furnace and heated up to 450 °C by following a strict temperature ramp. The temperatures and the heating steps were as described in Table 4.

TABLE 4. Standard sintering procedure (for both mesoporous and compact TiO_2)

Ramp (min)	5	15	5	5	60
Temp (°C)	125	325	375	450	150
Hold (min)	5	5	5	30	

3.1.5 Dye deposition

After the mesoporous layer, dyes were deposited by placing the substrates that were heated to 150 °C for 1 hour for moisture removal in advance and then cooled down to room temperature by blowing nitrogen, in the dye solution (0,1mM) that was also heated to 80 °C in order to improve solubility. The solution was left to 80 °C heat block for 24 hours and then dipped in the same solvent as the dye (1:1 toluene:ethanol v/v) 2 times.

3.1.6 Thermal evaporation of top electrode

Finally, the solar cell structures were completed with the top-electrode preparation, i.e. a silver (Ag) electrode. This was done by thermally evaporating silver pellets in a Edwards high-vacuum chamber (P = 10^{-6} mbar). Before the evaporation, they were masked to limit the active area of each solar cell to 0.1 cm^2. The thickness of the Ag electrode was 150 nm.

3.2. Characterization of solar cells

Solar cells were characterized after their fabrication by measuring their current-voltage (I-V) curves under simulated sunlight illumination (Picture 3) to calculate parameters

such as short-circuit current, open circuit voltage, fill factor and power conversion efficiency. The whole characterization, as well as the fabrication, took place in ambient air, without any encapsulation of the devices. Size of the active areas were accurately evaluated by an optical Dino-Lite AM4113ZTL microscope with 35X magnification. The I-V characterization was recorded over a half year period and the data were collected into a table, as described in next chapter.

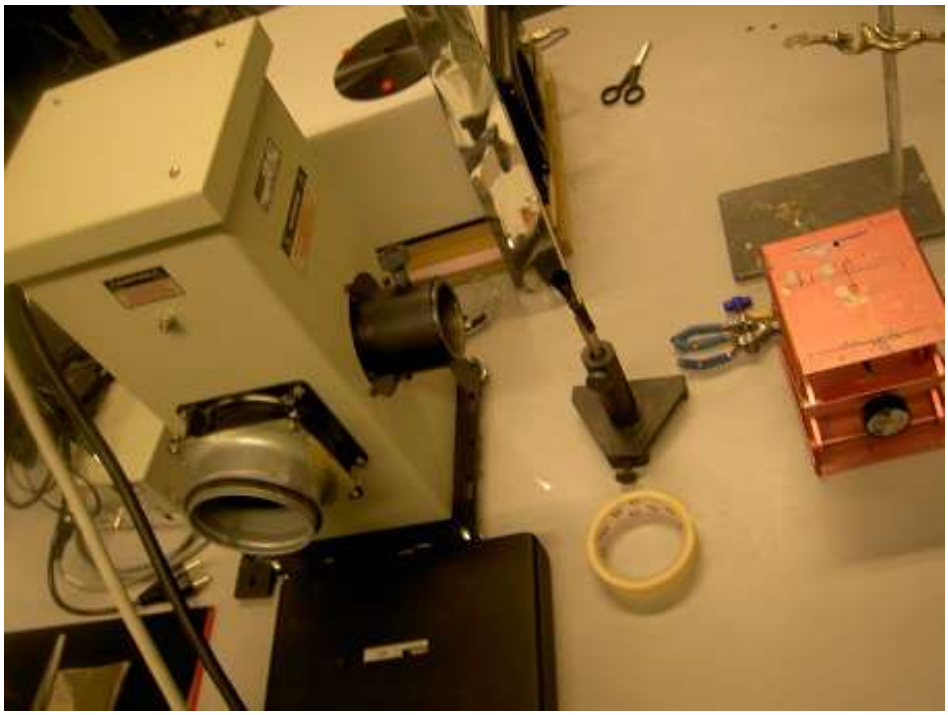

PICTURE 3: Solar simulator setup

Main error in the efficiency measurements derived from the lack of homogeneity of the illumation source. However, the light intensity was checked with a reference silicon solar cell before each set of measurements. Moreover, the purpose of this work is a relative comparison between the perylene dye-containing cells and those containing the ruthenium-dye. Thus, the error resulting from the unhomogeneous light source is negligible and not affecting the conclusions of this work.

4 RESULTS AND DISCUSSION

Efficiencies, open circuit voltages and also short circuit currents and fill factors of the best performing samples have been calculated from raw data of the I-V measurements which is presented in Appendix 1. Cells with most suitable properties for long-term use or which give the best responses still after a long time have been chosen for comparison for future research and their results have been presented as tables and charts of results.

Highest efficiencies measured for each sample, calculated from Appendix 1:

ZA96 (Sample 1, week 27/2015), highest η = 1,9 % (Sample 1, week 27/2015), remaining efficiency at 16.5.2016: 0,64 %

N719 (Sample 2, week 28/2015), highest η = 2,2 % (Sample 2, week 28/2015), remaining efficiency at 16.5.2016: η = 0,84 %

I-V curves for the champions cells, i.e. the best performing devices, containing the two compounds are depicted in Figure 9 and 10.

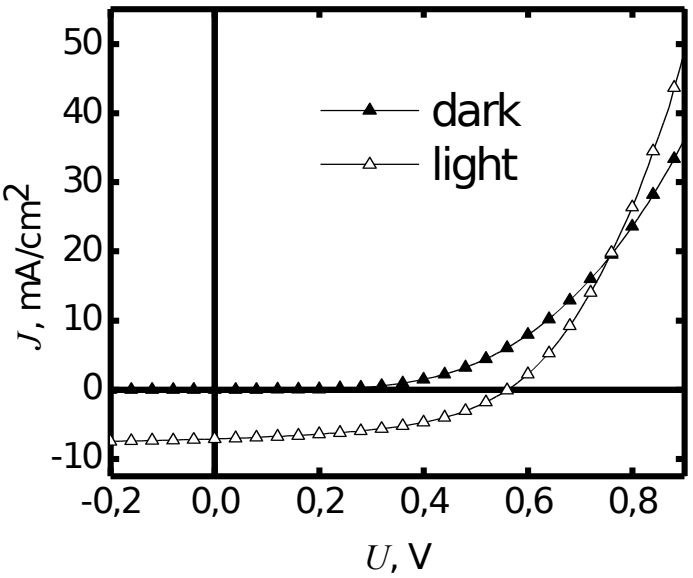

FIGURE 9: ZA96 solar cell I-V curve (Sample 1, week 27/2015)

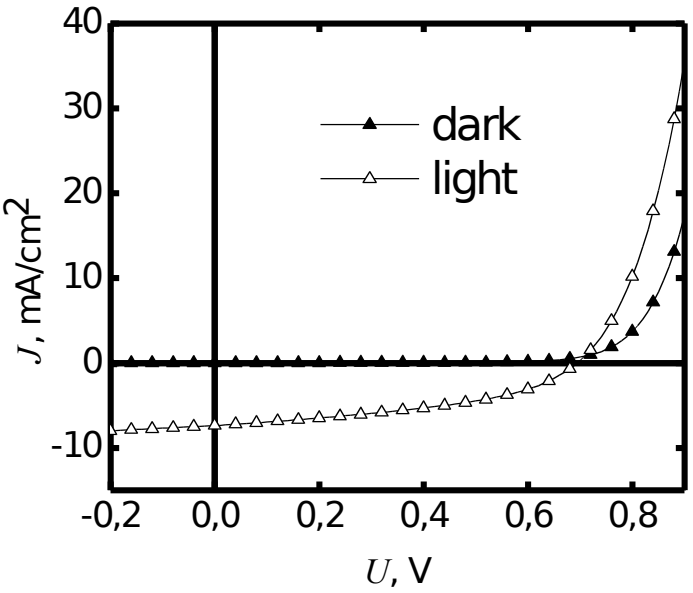

FIGURE 10: N719 solar cell I-V curve (Sample 2, week 28/2015)

As mentioned in theory part of this Thesis, the more square-like the shape of the IV-curve is, the better it performs in general. Both compounds have this property in their illuminated curve and show a quick rise in the current density from plus to minus only after 0,6 volts which indicates good open circuit voltage usually also leading to high efficiencies.

Calculated degradation parameters showed similar shape for most samples, presented below is the sample with most successful and highest quality measurements for degradation analysis, N719 (week 29, sample 2). All following results have been calculated from raw data presented in the end of Thesis with formulas and terms introduced in Chapter 2.1.

TABLE 5: Calculated efficiencies for N719 (week 28, sample 2)

	time, h	PCE, %
10.8.2015	1	1,98
13.8.2015	72	2,25
15.8.2015	120	1,91
17.7.2015	168	1,84
20.7.2015	240	1,94
27.7.2015	408	1,68
3.8.2015	576	1,87
10.8.2015	744	1,68
17.8.2015	912	1,42
25.8.2015	1104	1,34
31.8.2015	1255	1,33
15.9.2015	1615	1,40
10.3.2016	5857	1,06
5.4.2016	6481	0,96
16.5.2016	7489	0,84

FIGURE 11: Calculated efficiencies for N719 shown as chart (week 28, sample 2)

TABLE 6: N719 sample, calculated short circuit current density (week 28, sample 2)

	time, h	J_{SC}, mA/cm^2
10.7.2015	1	6,45
13.7.2015	72	7,38
15.7.2015	120	6,38
17.7.2015	168	5,91
20.7.2015	240	6,52
27.7.2015	408	5,73
3.8.2015	576	6,63
10.8.2015	744	5,90
17.8.2015	912	5,31
24.8.2015	1085	4,45
25.8.2015	1104	5,19
31.8.2015	1255	4,65
15.9.2015	1615	5,10
10.3.2016	5857	3,95
5.4.2016	6481	3,48
16.5.2016	7489	2,10

FIGURE 12: Calculated short circuit current density for N719 shown as chart (week 28, sample 2)

TABLE 7: N719 sample, calculated open circuit voltage (week 28, sample 2)

	time, h	U_{OC}, V
10.7.2015	1	0,67
13.7.2015	72	0,69
15.7.2015	120	0,68
17.7.2015	168	0,69
20.7.2015	240	0,68
27.7.2015	408	0,67
3.8.2015	576	0,66
10.8.2015	744	0,66
17.8.2015	912	0,63
25.8.2015	1104	0,61
31.8.2015	1255	0,65
15..9.2015	1615	0,64
10.3.2016	5857	0,58
5.4.2016	6481	0,59
16.5.2016	7489	0,58

FIGURE 13: Calculated open circuit voltage for N719 shown as chart (week 28, sample 2)

TABLE 8: N719 sample, calculated Fill factor (week 28, sample 2)

	time, h	FF
10.7.2015	1	0,45
13.7.2015	72	0,43
15.7.2015	120	0,43
17.7.2015	168	0,45
20.7.2015	240	0,43
27.7.2015	408	0,43
3.8.2015	576	0,42
10.8.2015	744	0,43
17.8.2015	912	0,42
25.8.2015	1104	0,42
31.8.2015	1255	0,44
15.9.2015	1615	0,43
10.3.2016	5857	0,46
5.4.2016	6481	0,47
16.5.2016	7489	0,68

FIGURE 14: Calculated fill factor for N719 shown as chart (week 28, sample 2)

Results show a rise to peak efficiency only after 2 to 3 days of time which is expected behavior for this type of cells. After this there can be observed a stable drop in every parameter over time which indicates the cells are clearly degrading in terms of efficiency and usability. Only Fill factor is showing higher numbers but this is only because it usually does not change from original state except when there are changes or defects forming in the cell inevitably leading to disfunction or short circuiting soon as is the case with this cell after around 8000 hours of lifetime.

Altough the lifetime of one year with over half of the maximum efficiency can be considered very long for research cells, it is still not enough to be considered usable for commercial purposes but it should be noted that in this case no kind of encapsulation of cells was applied which could in best case even dramatically increase the lifetime. It would be very interesting to see in future research how different kinds of transparent encapsulation materials with low light absorbtion like plastics could effect the degradation.

5 CONCLUSION

Aim of this Thesis was to analyse the performance of a novel perylene-based dye synthesized at Tampere University of Technology, ZA96, and compare it to the commercial and widely used ruthenium-dye N719. The perylene imide compound was found to be competitive with the ruthenium dye in terms of device efficiency and stability.

This may allow the replacement of the expensive N719 with cheaper and more environmental friendly perylene sensitizer for solid-state dye sensitized solar cells. Results show that ZA96 was able to reach almost the same efficiency (1.9%) as the commercial N719 dye, (2.2 %) which under optimization has been proven capable of reaching performance over 10%. Important to notice is also that ZA96 showed a slower degradation in most of the aging tests. The results are interesting since there has not been many alternative low-cost compounds capable of reaching the efficiency and stability of N719 standard dye.

The efficiencies achieved in this work are still modest. However, it is important to underline that no optimization of the different solar cell layer thicknesses had been carried out, and that the whole fabrication and characterization took place in ambient air. In order to reach and possibly overcome the state-of-the-art performances of solid state dye sensitized solar cells, further research is thus needed to optimize the fabrication conditions of the solar cells, starting from the promising results presented in this Thesis.

Much was learned about the operation and production of solar cells and how they are characterized and what laboratory work is involved in their research. Cleanroom work was also involved with methods not yet familiar from school like anhydrous solvent usage and a lot of small tasks inside and outside laboratory, including computer data processing.

6 REFERENCES

Aggeliki, K. 2011. Organic Solar Cells vs Semiconductor-based Solar Cells. Read 20.4.2015. http://www.brighthub.com/environment/renewable-energy/articles/95572.aspx

Bentor, Yinon. Chemical Element.com - Ruthenium. May 20, 2016. Read 20.4.2016 http://www.chemicalelements.com/elements/ru.html

DTU 2016, Technical University of Denmark 2016, Online course on solar cells

Halls J.J.M., Friend R.H. 2001. Clean electricity from photovoltaics. London: Imperial College Press.

IEA 2014 Snapshot of Global PV Markets, International Energy Agency report. Read 20.4.2016 http://www.iea-pvps.org/fileadmin/dam/public/report/technical/PVPS_report_-_A_Snapshot_of_Global_PV_-_1992-2014.pdf

Merhari, L. 2009. Hybrid Nanocomposites for Nanotechnology, Springer publishing

Saarinen, T. 2015. Hybrid organic–inorganic nanostructures for solar cells — a combined experimental and computational study, Thesis for the degree of Master of Science in Technology, Tampere University of Technology

Vivo, P. 2010. Multilayered Thin Films for Organic Photovoltaics, Thesis for the degree of Doctor of Science in Technology, Tampere University of Technology

7 APPENDICES

Appendix 1. Raw data examples from IV-measurements of 3 days used in calculation of efficiency and degradation results of ZA96 and N719

10 7 2015

week 27

S1_dark		S1_illuminated	
VA	IA	VA	IA
-0.2	-1.29E-06	-0.2	-2.80E-04
-0.19	-1.22E-06	-0.19	-2.79E-04
-0.18	-1.16E-06	-0.18	-2.80E-04
-0.17	-1.09E-06	-0.17	-2.79E-04
-0.16	-1.03E-06	-0.16	-2.79E-04
-0.15	-9.67E-07	-0.15	-2.79E-04
-0.14	-9.09E-07	-0.14	-2.79E-04
-0.13	-8.45E-07	-0.13	-2.79E-04
-0.12	-7.87E-07	-0.12	-2.78E-04
-0.11	-7.32E-07	-0.11	-2.79E-04
-0.1	-6.72E-07	-0.1	-2.78E-04
-0.09	-6.15E-07	-0.09	-2.78E-04
-0.08	-5.59E-07	-0.08	-2.76E-04
-0.07	-5.07E-07	-0.07	-2.76E-04
-0.06	-4.53E-07	-0.06	-2.75E-04
-0.05	-3.96E-07	-0.05	-2.75E-04
-0.04	-3.45E-07	-0.04	-2.74E-04
-0.03	-2.91E-07	-0.03	-2.73E-04
-0.02	-2.31E-07	-0.02	-2.73E-04
-0.01	-1.71E-07	-0.01	-2.71E-04
0	-1.07E-07	0	-2.71E-04
0.01	-3.60E-08	0.01	-2.70E-04
0.02	4.21E-08	0.02	-2.70E-04
0.03	1.32E-07	0.03	-2.68E-04
0.04	2.33E-07	0.04	-2.68E-04
0.05	3.51E-07	0.05	-2.66E-04
0.06	4.92E-07	0.06	-2.65E-04
0.07	6.59E-07	0.07	-2.64E-04
0.08	8.54E-07	0.08	-2.63E-04
0.09	1.09E-06	0.09	-2.62E-04
0.1	1.37E-06	0.1	-2.61E-04
0.11	1.71E-06	0.11	-2.60E-04
0.12	2.11E-06	0.12	-2.58E-04
0.13	2.59E-06	0.13	-2.57E-04
0.14	3.16E-06	0.14	-2.56E-04
0.15	3.85E-06	0.15	-2.54E-04
0.16	4.67E-06	0.16	-2.53E-04
0.17	5.62E-06	0.17	-2.51E-04
0.18	6.73E-06	0.18	-2.49E-04
0.19	8.04E-06	0.19	-2.48E-04
0.2	9.55E-06	0.2	-2.45E-04
0.21	1.13E-05	0.21	-2.45E-04
0.22	1.33E-05	0.22	-2.42E-04
0.23	1.56E-05	0.23	-2.40E-04
0.24	1.83E-05	0.24	-2.38E-04

week 28

S2_dark		S2_illuminated	
VA	IA	VA	IA
-0.2	-1.32E-06	-0.2	-3.03E-04
-0.19	-1.24E-06	-0.19	-3.01E-04
-0.18	-1.14E-06	-0.18	-3.00E-04
-0.17	-1.04E-06	-0.17	-2.98E-04
-0.16	-9.50E-07	-0.16	-2.97E-04
-0.15	-8.52E-07	-0.15	-2.96E-04
-0.14	-7.65E-07	-0.14	-2.94E-04
-0.13	-6.79E-07	-0.13	-2.93E-04
-0.12	-6.01E-07	-0.12	-2.93E-04
-0.11	-5.32E-07	-0.11	-2.91E-04
-0.1	-4.71E-07	-0.1	-2.90E-04
-0.09	-4.14E-07	-0.09	-2.90E-04
-0.08	-3.62E-07	-0.08	-2.88E-04
-0.07	-1.95E-07	-0.07	-2.87E-04
-0.06	-1.56E-07	-0.06	-2.86E-04
-0.05	-1.25E-07	-0.05	-2.85E-04
-0.04	-9.67E-08	-0.04	-2.84E-04
-0.03	-7.14E-08	-0.03	-2.83E-04
-0.02	-5.24E-08	-0.02	-2.82E-04
-0.01	-3.49E-08	-0.01	-2.80E-04
0	-1.89E-08	0	-2.80E-04
0.01	-6.70E-09	0.01	-2.77E-04
0.02	6.56E-09	0.02	-2.76E-04
0.03	1.71E-08	0.03	-2.75E-04
0.04	2.81E-08	0.04	-2.74E-04
0.05	3.98E-08	0.05	-2.72E-04
0.06	4.71E-08	0.06	-2.71E-04
0.07	5.36E-08	0.07	-2.70E-04
0.08	6.27E-08	0.08	-2.68E-04
0.09	7.02E-08	0.09	-2.67E-04
0.1	7.80E-08	0.1	-2.66E-04
0.11	8.77E-08	0.11	-2.64E-04
0.12	1.00E-07	0.12	-2.62E-04
0.13	1.09E-07	0.13	-2.61E-04
0.14	1.19E-07	0.14	-2.59E-04
0.15	1.29E-07	0.15	-2.58E-04
0.16	1.38E-07	0.16	-2.56E-04
0.17	1.48E-07	0.17	-2.55E-04
0.18	1.60E-07	0.18	-2.53E-04
0.19	1.72E-07	0.19	-2.52E-04
0.2	1.86E-07	0.2	-2.50E-04
0.21	2.00E-07	0.21	-2.48E-04
0.22	2.13E-07	0.22	-2.45E-04
0.23	2.30E-07	0.23	-2.44E-04
0.24	2.43E-07	0.24	-2.42E-04

20 7 2015

week 27

S1_dark		S1_illuminated	
VA	IA	VA	IA
-0.2	-6.45E-07	-0.2	-3.01E-04
-0.19	-6.17E-07	-0.19	-3.00E-04
-0.18	-5.95E-07	-0.18	-2.99E-04
-0.17	-5.74E-07	-0.17	-2.99E-04
-0.16	-5.49E-07	-0.16	-2.99E-04
-0.15	-5.21E-07	-0.15	-2.99E-04
-0.14	-4.97E-07	-0.14	-2.98E-04
-0.13	-4.77E-07	-0.13	-2.97E-04
-0.12	-4.55E-07	-0.12	-2.98E-04
-0.11	-4.29E-07	-0.11	-2.97E-04
-0.1	-4.03E-07	-0.1	-2.96E-04
-0.09	-3.81E-07	-0.09	-2.97E-04
-0.08	-3.59E-07	-0.08	-2.95E-04
-0.07	-3.34E-07	-0.07	-2.95E-04
-0.06	-3.07E-07	-0.06	-2.94E-04
-0.05	-2.80E-07	-0.05	-2.94E-04
-0.04	-2.57E-07	-0.04	-2.92E-04
-0.03	-2.31E-07	-0.03	-2.92E-04
-0.02	-2.00E-07	-0.02	-2.90E-04
-0.01	-1.63E-07	-0.01	-2.90E-04
0	-1.28E-07	0	-2.89E-04
0.01	-8.68E-08	0.01	-2.88E-04
0.02	-3.89E-08	0.02	-2.86E-04
0.03	1.68E-08	0.03	-2.86E-04
0.04	8.42E-08	0.04	-2.84E-04
0.05	1.62E-07	0.05	-2.84E-04
0.06	2.57E-07	0.06	-2.82E-04
0.07	3.74E-07	0.07	-2.81E-04
0.08	5.13E-07	0.08	-2.80E-04
0.09	6.82E-07	0.09	-2.79E-04
0.1	8.86E-07	0.1	-2.78E-04
0.11	1.14E-06	0.11	-2.76E-04
0.12	1.44E-06	0.12	-2.76E-04
0.13	1.79E-06	0.13	-2.73E-04
0.14	2.22E-06	0.14	-2.72E-04
0.15	2.72E-06	0.15	-2.70E-04
0.16	3.32E-06	0.16	-2.69E-04
0.17	4.03E-06	0.17	-2.66E-04
0.18	4.86E-06	0.18	-2.65E-04
0.19	5.83E-06	0.19	-2.64E-04
0.2	6.96E-06	0.2	-2.61E-04
0.21	8.26E-06	0.21	-2.59E-04
0.22	9.76E-06	0.22	-2.58E-04
0.23	1.15E-05	0.23	-2.57E-04
0.24	1.35E-05	0.24	-2.53E-04

week 28

S2_dark		S2_illuminated	
VA	IA	VA	IA
-0.2	-6.76E-07	-0.2	-3.06E-04
-0.19	-6.39E-07	-0.19	-3.05E-04
-0.18	-6.02E-07	-0.18	-3.04E-04
-0.17	-5.58E-07	-0.17	-3.03E-04
-0.16	-5.12E-07	-0.16	-3.02E-04
-0.15	-4.76E-07	-0.15	-3.01E-04
-0.14	-4.43E-07	-0.14	-3.00E-04
-0.13	-4.07E-07	-0.13	-2.98E-04
-0.12	-3.73E-07	-0.12	-2.97E-04
-0.11	-3.48E-07	-0.11	-2.96E-04
-0.1	-3.25E-07	-0.1	-2.95E-04
-0.09	-3.00E-07	-0.09	-2.94E-04
-0.08	-2.79E-07	-0.08	-2.93E-04
-0.07	-2.66E-07	-0.07	-2.91E-04
-0.06	-2.53E-07	-0.06	-2.90E-04
-0.05	-2.36E-07	-0.05	-2.89E-04
-0.04	-2.23E-07	-0.04	-2.88E-04
-0.03	-2.15E-07	-0.03	-2.86E-04
-0.02	-2.06E-07	-0.02	-2.85E-04
-0.01	-1.94E-07	-0.01	-2.83E-04
0	-1.86E-07	0	-2.82E-04
0.01	-1.83E-07	0.01	-2.80E-04
0.02	-1.77E-07	0.02	-2.79E-04
0.03	-1.66E-07	0.03	-2.77E-04
0.04	-1.61E-07	0.04	-2.76E-04
0.05	-1.57E-07	0.05	-2.75E-04
0.06	-1.50E-07	0.06	-2.73E-04
0.07	-1.41E-07	0.07	-2.72E-04
0.08	-1.36E-07	0.08	-2.70E-04
0.09	-1.33E-07	0.09	-2.68E-04
0.1	-1.26E-07	0.1	-2.67E-04
0.11	-1.16E-07	0.11	-2.65E-04
0.12	-1.11E-07	0.12	-2.63E-04
0.13	-1.04E-07	0.13	-2.62E-04
0.14	-9.09E-08	0.14	-2.60E-04
0.15	-8.51E-08	0.15	-2.58E-04
0.16	-7.78E-08	0.16	-2.56E-04
0.17	-6.88E-08	0.17	-2.55E-04
0.18	-5.55E-08	0.18	-2.53E-04
0.19	-4.31E-08	0.19	-2.51E-04
0.2	-3.26E-08	0.2	-2.48E-04
0.21	-2.29E-08	0.21	-2.47E-04
0.22	-1.12E-08	0.22	-2.44E-04
0.23	1.15E-10	0.23	-2.43E-04
0.24	1.42E-08	0.24	-2.40E-04

25 8 2015

week 27

S1_dark		S1_illuminated	
VA	IA	VA	IA
-0.2	-4.80E-07	-0.2	-2.81E-04
-0.19	-4.67E-07	-0.19	-2.80E-04
-0.18	-4.49E-07	-0.18	-2.80E-04
-0.17	-4.28E-07	-0.17	-2.80E-04
-0.16	-4.14E-07	-0.16	-2.79E-04
-0.15	-4.03E-07	-0.15	-2.79E-04
-0.14	-3.85E-07	-0.14	-2.77E-04
-0.13	-3.67E-07	-0.13	-2.78E-04
-0.12	-3.50E-07	-0.12	-2.77E-04
-0.11	-3.32E-07	-0.11	-2.75E-04
-0.1	-3.12E-07	-0.1	-2.76E-04
-0.09	-2.90E-07	-0.09	-2.74E-04
-0.08	-2.79E-07	-0.08	-2.74E-04
-0.07	-2.65E-07	-0.07	-2.73E-04
-0.06	-2.44E-07	-0.06	-2.72E-04
-0.05	-2.26E-07	-0.05	-2.71E-04
-0.04	-2.05E-07	-0.04	-2.70E-04
-0.03	-1.82E-07	-0.03	-2.69E-04
-0.02	-1.55E-07	-0.02	-2.69E-04
-0.01	-1.35E-07	-0.01	-2.67E-04
0	-1.08E-07	0	-2.66E-04
0.01	-7.14E-08	0.01	-2.66E-04
0.02	-3.48E-08	0.02	-2.64E-04
0.03	4.77E-09	0.03	-2.63E-04
0.04	5.83E-08	0.04	-2.63E-04
0.05	1.16E-07	0.05	-2.61E-04
0.06	1.91E-07	0.06	-2.61E-04
0.07	2.81E-07	0.07	-2.59E-04
0.08	3.81E-07	0.08	-2.58E-04
0.09	5.03E-07	0.09	-2.57E-04
0.1	6.55E-07	0.1	-2.55E-04
0.11	8.33E-07	0.11	-2.54E-04
0.12	1.05E-06	0.12	-2.53E-04
0.13	1.31E-06	0.13	-2.51E-04
0.14	1.61E-06	0.14	-2.51E-04
0.15	1.97E-06	0.15	-2.49E-04
0.16	2.39E-06	0.16	-2.47E-04
0.17	2.88E-06	0.17	-2.46E-04
0.18	3.46E-06	0.18	-2.45E-04
0.19	4.12E-06	0.19	-2.42E-04
0.2	4.89E-06	0.2	-2.40E-04
0.21	5.77E-06	0.21	-2.39E-04
0.22	6.77E-06	0.22	-2.37E-04
0.23	7.91E-06	0.23	-2.35E-04
0.24	9.21E-06	0.24	-2.34E-04

week 28

S2_dark		S2_illuminated	
VA	IA	VA	IA
-0.2	-3.61E-07	-0.2	-2.46E-04
-0.19	-3.61E-07	-0.19	-2.45E-04
-0.18	-3.44E-07	-0.18	-2.44E-04
-0.17	-3.34E-07	-0.17	-2.44E-04
-0.16	-3.30E-07	-0.16	-2.43E-04
-0.15	-3.17E-07	-0.15	-2.42E-04
-0.14	-3.02E-07	-0.14	-2.42E-04
-0.13	-2.89E-07	-0.13	-2.40E-04
-0.12	-2.76E-07	-0.12	-2.40E-04
-0.11	-2.58E-07	-0.11	-2.38E-04
-0.1	-2.48E-07	-0.1	-2.37E-04
-0.09	-2.45E-07	-0.09	-2.36E-04
-0.08	-2.35E-07	-0.08	-2.35E-04
-0.07	-2.24E-07	-0.07	-2.34E-04
-0.06	-2.14E-07	-0.06	-2.33E-04
-0.05	-2.05E-07	-0.05	-2.32E-04
-0.04	-1.91E-07	-0.04	-2.31E-04
-0.03	-1.85E-07	-0.03	-2.31E-04
-0.02	-1.85E-07	-0.02	-2.28E-04
-0.01	-1.79E-07	-0.01	-2.26E-04
0	-1.73E-07	0	-2.24E-04
0.01	-1.66E-07	0.01	-2.25E-04
0.02	-1.59E-07	0.02	-2.23E-04
0.03	-1.48E-07	0.03	-2.21E-04
0.04	-1.73E-07	0.04	-2.21E-04
0.05	-1.47E-07	0.05	-2.19E-04
0.06	-1.40E-07	0.06	-2.17E-04
0.07	-1.33E-07	0.07	-2.16E-04
0.08	-1.22E-07	0.08	-2.14E-04
0.09	-1.29E-07	0.09	-2.12E-04
0.1	-1.20E-07	0.1	-2.11E-04
0.11	-1.13E-07	0.11	-2.09E-04
0.12	-1.06E-07	0.12	-2.08E-04
0.13	-1.03E-07	0.13	-2.06E-04
0.14	-9.83E-08	0.14	-2.04E-04
0.15	-9.18E-08	0.15	-2.03E-04
0.16	-8.41E-08	0.16	-2.01E-04
0.17	-7.82E-08	0.17	-1.99E-04
0.18	-7.08E-08	0.18	-1.97E-04
0.19	-6.48E-08	0.19	-1.96E-04
0.2	-5.77E-08	0.2	-1.94E-04
0.21	-4.91E-08	0.21	-1.92E-04
0.22	-4.48E-08	0.22	-1.91E-04
0.23	-3.27E-08	0.23	-1.88E-04
0.24	-2.51E-08	0.24	-1.87E-04